

Project Narrative

1 Significance of Project

Core-collapse supernovae (CCSNe) are the most extreme laboratories for nuclear physics in the universe. Stellar core collapse and the violent explosions that follow give birth to neutron stars and black holes, and in the process synthesize most of the elements heavier than helium throughout the universe. The behavior of matter at supranuclear densities is crucial to the CCSN mechanism, as are strong and weak interactions. Beyond Standard Model behavior of neutrinos may also impact the CCSN mechanism. Despite the key role CCSNe play in many aspects of astrophysics, and decades of research effort, *we still do not fully understand the details of the physical mechanism that causes these explosions*. This leaves frustratingly large error bars on many key aspects of our theoretical understanding of the universe, and also makes it difficult to constrain uncertain nuclear physics with data from CCSNe.

We propose an end-to-end, multi-year investigation of CCSNe that includes the effects of rotation, magnetic fields, and progenitor asphericity. Our comprehensive research program will consist of 3D MHD CCSN simulations with sophisticated multi-dimensional neutrino transport, the most realistic initial conditions ever adopted for the study of CCSNe, and an intensive comparison to observations through the calculation of gravitational wave emission, detailed nucleosynthesis, and electromagnetic radiative transfer. The ambitious objectives of this project will be achievable by leveraging the unique combination of skills in the proposal team, cutting-edge open-source software, and the Leadership-class resources available through the INCITE program.

1.1 Achievements with Previous INCITE Allocation

The PI is also PI of the 2015-2017 INCITE allocation “Petascale Simulation of Magnetorotational Core-collapse Supernovae.” Based on simulations performed during Year 1 of that project, we have shown that modest rotation and magnetic fields can have a significant impact on the CCSN mechanism, both acting to lower the threshold to explosion in 3D. Additionally, using extremely high-resolution simulations of MHD turbulence in the CCSN gain region carried out as part of that project, we demonstrated that the gain region is also unstable to growth of the magnetorotational instability (MRI), implying exponential growth of magnetic field strengths and potential important impact on the rate of turbulent dissipation (e.g., [Thompson et al. 2005](#)). Regions of MRI growth in the entire post-shock region are shown in the left panel of Figure 1.

During Year 2 of that INCITE project, we carried out high-resolution 3D simulations of CCSNe with multidimensional M1 neutrino transport. These simulations have shown the presence of the standing accretion shock instability (SASI) and have shown that progenitor perturbations can aid shock expansion (middle panel of Figure 1). By 500 ms, however, we have yet to see the initiation of an explosion in any of our models. A few of the most promising cases are being continued to later times at present.

During Year 3 of the previous INCITE allocation, we are running 3D MHD CCSN simulations including M1 neutrino transport. These simulations are just now getting underway but will serve as crucial pre-cursors to the simulations we plan in the present proposal.

Several publications on the results of our simulations from the previous INCITE allocation are currently in preparation or already under review.

1.2 Background

Despite over a half-century of theoretical and computational effort, the detailed nature of the mechanism that reverses stellar core collapse and drives robust CCSN explosions remains uncertain. In the final stages of nuclear burning, massive stars form inert iron cores. These iron cores grow via silicon shell burning to beyond their maximum stable mass, the effective Chandrasekhar limit, at which point gravitational collapse ensues. This collapse is accelerated by ever-increasing neutrino cooling, photodissociation of iron nuclei, and electron captures onto protons. The collapse proceeds until the central regions of the core exceed nuclear density. At such small inter-nucleon spacings, the strong nuclear force becomes repulsive and dramatically

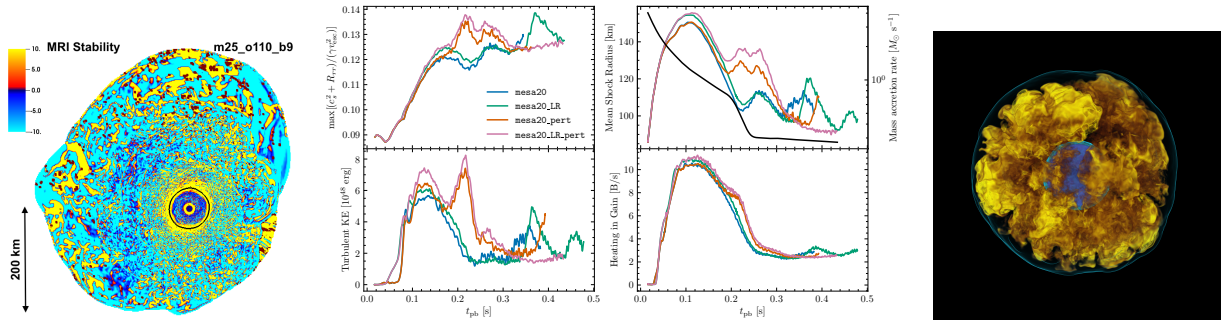


Figure 1: **Left:** Regions of instability to the MRI in a 3D CCSN simulation. Blue regions indicating growth of the MRI. **Center:** Results for 3D M1 neutrino transport simulations in a $20-M_\odot$ star. **Right:** Volume rendering of entropy from a 3D CCSN simulation with M1 neutrino transport.

halts the collapse. This effective stiffening of the equation of state launches a strong shock wave into the still collapsing outer part of iron core. Early calculations of this process in spherical symmetry suggested that this “bounce” shock would be sufficiently energetic to unbind the outer parts of the collapsing star and power the supernova explosion (Colgate et al. 1961). But it was quickly realized that catastrophic neutrino cooling behind the shock and photodissociation of the infall iron nuclei by the shock would lead to an enormous amount of energy loss causing the shock to stall.

The over-arching goal of the theoretical investigation of the CCSN mechanism is to make *explanatory* and *predictive* connection to observation and experiment. Doing this in a rigorous way requires a successful, physically accurate model for the explosion mechanism. Even studies of stellar nucleosynthesis from massive stars (e.g., Woosley & Weaver 1995; Woosley & Heger 2007), which arguably only require that an energetic explosion occur in massive stars, are limited to studying only low mass nuclei since the high mass nuclei can only be synthesized deep within the explosion where the details of the mechanism play a crucial role. Any investigation of high-mass element formation (i.e., the r-process) in CCSNe requires a self-consistent model for the explosion mechanism. This is a critical need for connecting nuclear astrophysics to current and future experimental efforts at, e.g., JLAB, RHIC, NSCL, FRIB, etc. Armed with 21st-century tools, the solution to this problem that has been vexing us since the 20th century may finally be within reach. Successful, energetic explosions across an adequate range of progenitor star masses may hinge on 3D hydrodynamics that captures the correct behavior of turbulence, general relativistic gravity, accurate energy-dependent neutrino transport, sophisticated microphysics based on modern nuclear theory, and realistic stellar progenitor models that directly model the truly 3D structure of massive stars (e.g., Meakin & Arnett 2007; Arnett & Meakin 2011; Couch et al. 2015).

All stars rotate and have magnetic fields. Following massive star core collapse, rapid rotation and strong magnetic fields can lead to powerful outflows from the PNS (Wheeler et al. 2000, 2002; Burrows et al. 2007; Winteler et al. 2012) that were first suggested as a possible CCSN explosion mechanism by LeBlanc & Wilson (1970). Such magnetically-driven explosions are an interesting possibility for r-process nucleosynthesis (Winteler et al. 2012). With MHD energy deposition driving the PNS wind, the potential for neutrinos to remove the needed neutron-richness is reduced, enhancing the possibility for the main r-process to be produced in (some) SN. Modern stellar evolution calculations, however, indicate that diffusive mixing and magnetic braking effects efficiently transport angular momentum out from massive stellar cores (Spruit 2002; Heger et al. 2005; Paxton et al. 2013). Given the observed distribution of initial rotation speeds of massive stars, this strongly indicates that the vast majority of massive stellar cores at collapse do not rotate rapidly enough to lead to magnetorotational explosions. It is likely that magnetorotational effects play a dominant role in only $\sim 1\%$ of all core collapse events, corresponding to the fraction of Long Gamma-ray Bursts (LGRBs) and so-called broad line Type Ic SNe (Modjaz et al. 2016). However, this rarity is not

inconsistent with the GCE evidence for the main r-process source.

We know, however, that highly magnetized neutron stars known as magnetars are not that uncommon, accounting for about 10% of the neutron star population. This points to a generic mechanism in stellar collapse that results in strong magnetic fields in the compact remnant some significant fraction of the time. Additionally, we know there are mechanisms that can amplify even initially very weak magnetic fields with exponential growth rates. Akiyama et al. (2003) pointed out that a collapsing stellar core is generically unstable to growth of the magnetorotational instability (MRI) (Chandrasekhar 1961; Balbus & Hawley 1991). The MRI grows exponentially on the rotational time scale and taps the energy of differential rotation to amplify the magnetic field and drive turbulence. Turbulence has been shown to play a leading-order role in driving the dynamics of the stalled SN shock and explosion (Burrows & Hayes 1996; Murphy et al. 2013; Couch & Ott 2013, 2015). Even in non-rapidly rotating stellar cores, magnetic fields could be amplified to strengths that could qualitatively change the behavior of the turbulence in the post-shock gain layer as well as lead to enhance turbulent dissipation to heat, which can also aid explosion (e.g., Thompson et al. 2005; Ott et al. 2006).

As part of this INCITE project, we will extensively explore the conditions that could lead to magnetar formation through 3D CCSN simulations of rotating and magnetic progenitor stars. Our primary tool for this exploration will be FLASH, which implements a state-of-the-art high-order MHD solver in an AMR framework. We will explore a range of realistic initial rotation profiles and magnetic field strengths based on stellar evolution calculations that include prescriptions for rotation, magnetic field amplification, and angular momentum transport (e.g., Heger et al. 2005; Paxton et al. 2013, 2015). This work will build on current studies underway using FLASH being executed by as part of a current DOE INCITE project. The proposed simulations and computational research will directly support the scientific goals of the DOE Early Career Research Award project DE-SC0015904 to PI Couch. Additionally, the proposed INCITE allocation would be used to support the research goals of a pending DOE SciDAC proposal “Toward Exascale Astrophysics of Mergers and Supernovae (TEAMS)”, lead-PI W. Raph Hix, Oak Ridge National Lab. PI Couch is the MSU PI for this SciDAC proposal and a member of the executive governing committee.

We will explore how rotation and magnetic fields can modify the behavior of post-shock turbulence in the CCSN context. Capturing turbulence in CCSN can be extremely demanding computationally (Abdikamalov et al. 2015; Couch & Ott 2015; Radice et al. 2015, 2016). This is particularly the case for turbulence-driving instabilities such as the magnetorotational instability (MRI), where the fastest growing mode in the CCSN context can be on the order of tens of meters (c.f., Akiyama et al. 2003; Burrows et al. 2007; Obergaulinger et al. 2009; Mösta et al. 2015). Thus, we propose a multi-pronged approach to studying magnetorotational turbulence in CCSNe. First, we will carry out simplified physics simulations in reduced domains small enough the MHD turbulence can be simulated directly (e.g., Obergaulinger et al. 2009; Mösta et al. 2015). Second, we will explore new numerical methods and algorithms for simulating MHD turbulence that have never before been applied to the CCSN context. This will include exploration of sub-grid turbulence models such as large-eddy closures (Pope 2000) and very high-order methods for MHD (Rembiasz et al. 2016) that are better able to capture the correct behavior of the turbulent cascade at finite resolution.

With the resulting substantially improved models, we will explore the implications for nucleosynthesis from magnetorotational CCSNe and newborn magnetars by computing the post-processing nuclear yields from tracer particles included in our 3D MHD CCSN simulations. From these calculations, will enable a greatly improved understanding of the role these sites play in the origin of the r-process nuclei.

1.3 Broader Impacts Through Open-Source Scientific Software

Our proposed project makes extensive use of open-source scientific software. Most notable is FLASH, a standard-bearer in open-source computational science that has contributed to nearly 1000 publications over the last 15 years, or so. Through efforts of the last few years, project team members led by Couch have greatly extended the capabilities of FLASH in order to treat the physics of CCSNe with high-fidelity. Most

of these code extensions have already been publicly released as part of FLASH. Additionally, our project will leverage the open-source, 1D GR CCSN code GR1D (O’Connor & Ott 2010, 2013; O’Connor 2015). Even the microphysics we employ in our simulations is based on open-source software: our flexible, tabular nuclear equation of state¹ and our neutrino opacities and emissivities, NuLib². Our dedication to open-source scientific software will be a central part of our project. We aim to not only foster scientific progress for those who might benefit from the software we develop but we also feel that openness is critical to a clear and forthright scientific discourse.

2 Research Objectives and Milestones

We propose a multi-year progressive investigation of the CCSN mechanism using realistic initial conditions. This project will develop and employ 3D massive stellar progenitor models at the point of core-collapse, including rotation and magnetic fields. We will address the critically important questions of whether rotation and magnetic fields aid successful explosions for “normal” CCSNe and how rotation and magnetic fields effect the nucleosynthesis in CCSNe. Our results will directly inform our understanding of the characteristics of newborn pulsars and magnetars, information that can be directly compared to observational data.

Our project will address two critical questions: How do plausible rotation rates and magnetic field strengths influence the CCSN mechanism? and What is the impact of realistic 3D progenitor structure including rotation and magnetic fields on the CCSN mechanism and observables?

2.1 The Spark-M1 CCSN Application

Our primary research software instrument for this project will be the Spark-M1 CCSN application built in the FLASH simulation framework (Fryxell et al. 2000; Dubey et al. 2009). Spark-M1 utilizes the new Spark high-order MHD solver (Couch 2017), the M1 two-moment explicit neutrino transport method (Shibata et al. 2011; O’Connor 2015; O’Connor & Couch 2015), an accurate and efficient multipole gravity solver (Couch et al. 2013) including the general relativistic monopole correction (Marek et al. 2006), an approximate 21-isotope nuclear network for accurately tracking the composition at low densities (Couch et al. 2015), and the FLASH framework for adaptive mesh refinement (AMR), I/O, and runtime management. The methods and physics including in Spark-M1 make it one of the most high-fidelity and high-performance CCSN simulation tools in the world. A detailed analysis of the performance characteristics of Spark-M1 is given in Section 3.3. In the remainder of this subsection we briefly described the numerical approach used in Spark-M1.

The Spark MHD solver (Couch 2017) implements the cell-centered method of generalized Lagrangian multipliers (GLM; Dedner et al. 2002; Mignone et al. 2010) to control the growth of the divergence of the magnetic field. The GLM-MHD scheme employs hyperbolic advection and parabolic damping of divergence errors in order to avoid expensive elliptic divergence cleaning (e.g., Jiang & Wu 1999) or complicated staggered-mesh constrained transport (e.g., Gardiner & Stone 2005; Lee & Deane 2009; Lee 2013). Spark implements the GLM-MHD scheme via a finite-volume approach using high-order primitive reconstruction, multiple Riemann solvers for flux calculation, and method-of-lines time integration using multi-stage strong stability preserving (SSP) low-storage Runge-Kutta (RK) integrators of second- and third-order (e.g., Gottlieb & Shu 1998). For realistic, non-Gamma-law equations of state, Spark avoids the approach of Colella & Glaz (1985) used in other FLASH solvers and adopts the volumetric internal energy, ρe , as an auxiliary thermodynamic primitive variable instead, as in Almgren et al. (2010). We have found this approach to be generally more robust but either method should be technically equivalent (e.g., Zingale & Katz 2015). For our CCSN application, we use fifth-order WENO reconstruction (Borges et al. 2008), second-order time integration, and the HLLD approximate Riemann solver which includes MHD waves (Miyoshi & Kusano 2005).

¹<http://stellarcollapse.org/equationofstate>

²<http://github.com/evanoc Connor/NuLib>

Neutrino transport in Spark–M1 is carried out using the M1 two-moment explicit approach described in O’Connor (2015); O’Connor & Couch (2015); O’Connor et al. (2017). The M1 scheme evolves the first two angular moments of the Boltzmann distribution function for neutrinos and utilizes an analytic closure for the higher-order moments. The neutrino fluxes, both in real space and in energy space, are computed explicitly as a hyperbolic system resulting in favorable performance and scaling properties (at the cost of time step sizes limited by the speed of light) while the matter-radiation source terms are computed implicitly. This implicit solve is completely local and requires solving only a 4x4 matrix. Our M1 solver is fully velocity-dependent, except in the calculation of the explicit flux terms, which is done to $\mathcal{O}(v/c)$. We currently do not include inelastic neutrino scattering in the multidimensional version of our transport solver although inelastic neutrino electron scattering is included in the 1D implementation in GR1D (O’Connor 2015). We plan to implement and include inelastic scattering in our 3D simulations in Years 2 and 3 of this project.

The two-moment M1 approach is inherently more accurate than zeroth-moment only approaches such as flux-limited diffusion (e.g., Bruenn et al. 2013; Dolence et al. 2015; Lentz et al. 2015). M1 does not require a flux-limiter-based closure for the radiation fluxes as they are solved for directly. Furthermore, the analytic closure we currently use for the moments beyond the first is simple and straightforward yet shows encouraging agreement with 1D Boltzmann and Monte Carlo neutrino transport calculations (O’Connor 2015; Murchikova et al. 2017). As compared with flux-limited diffusion, M1 does not suffer from the inability to capture “shadows” inherent to FLD schemes. A known limitation of M1 is cases in which distinct beams of radiation intersect, causing radiation “shocks.” The M1 solution in such cases becomes highly diffuse at the intersection. This is a problem in, e.g., radiation hydrodynamic calculations of accretion disks. For CCSNe, however, the radiation field is highly forward peaked and cases in which distinct beams of radiation might cross are essentially non-existent. Hence, M1 is *ideally* suited for the CCSN problem due to its accuracy (for the specific problem) and efficiency. In addition, the severe limitation of time steps determined by the speed of light is not so drastic in CCSNe since the explicit time step is already just a factor of a few larger than this thanks to the enormous sound speeds in the PNS. Another significant advantage of M1 is that it is a fully multidimensional transport scheme, i.e., the solution at a given grid point is dependent on the fluxes from every direction around that point. This is distinct from the often-adopted “ray-by-ray” approximation (e.g., Bruenn et al. 2013, 2016; Müller et al. 2012; Hanke et al. 2013; Melson et al. 2015; Lentz et al. 2015) in which the transport problem is solved only along discrete radial rays. The advantages of M1 for neutrino transport in CCSNe have not gone unnoticed and a number of groups are now exploring or adopting this approach (Just et al. 2015; Kuroda et al. 2016; Skinner et al. 2016; Roberts et al. 2016).

In our FLASH CCSN application we have assumed that the composition of the matter throughout the entire computational domain is determined by nuclear statistical equilibrium (NSE). This common approximation (e.g., Burrows et al. 2007; Ott et al. 2008; Dolence et al. 2015; Skinner et al. 2016; Roberts et al. 2016; Kuroda et al. 2016) is appropriate at high densities and temperatures where the nuclear reaction rates are sufficiently fast to establish equilibrium essentially instantly but becomes increasingly incorrect at low densities such as those in the silicon and oxygen shells surrounding the collapsing iron core. Critically, correctly predicting the explosion energy or nucleosynthetic products such as radioactive nickel can be severely impacted by the inappropriate assumption of NSE (Bruenn et al. 2016). Bruenn et al. (2016) advocate the use of an approximate nuclear network in regions that are not in NSE, while other groups (e.g., Müller et al. 2012; Melson et al. 2015) use a “flashing” approach rather than a full network calculation. We have recently implemented a method for transitioning to a nuclear network and appropriate EOS at low densities. Our new approach blends the pressures between the high- and low-density EOS’s to prevent spurious pressure discontinuities and uses an auxiliary variable to track whether a zone is entering or exiting NSE, allowing us to appropriately set the composition in the transition region.

Our use of high-order accurate methods can have tremendous advantages in correctly capturing the turbulent dynamics of the CCSN mechanism (Radice et al. 2015). Rembiasz et al. (2016) give a detailed analysis of the benefits of high-order methods for astrophysical MHD. They present an approach for directly

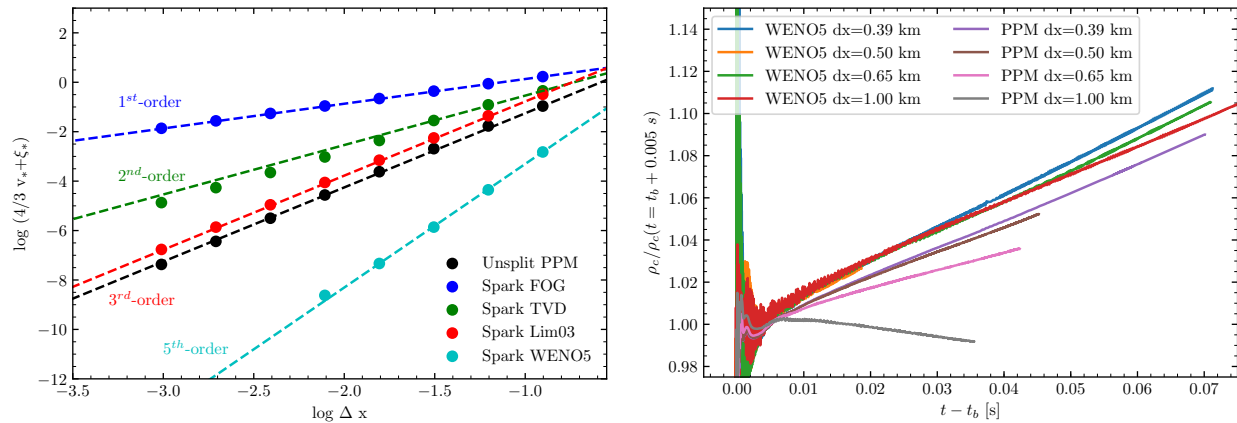


Figure 2: **Top:** Rate of convergence of the numerical viscosity with grid resolution in a multidimensional sound wave advection test for Spark with various spatial reconstruction schemes along with that of FLASH’s unsplit PPM solver. For these tests, the time step CFL factor was set to 0.01 so that the truncation error second-order time integration scheme used in all cases was small. **Bottom:** Post-bounce evolution of the normalized central density from 1D CCSN simulations at various resolutions for Spark with WENO5 and FLASH’s unsplit PPM solver. The higher-order accuracy of WENO5 allows the neutron star to be held gravitationally at lower resolution than for PPM.

measuring the effective numerical viscosity of a particular MHD solver. The numerical viscosity is directly related to the truncation error (i.e., accuracy) of a numerical scheme. In Figure 2 we show the effective numerical viscosity as a function of grid resolution for Spark using various difference spatial reconstruction schemes. We also show the numerical viscosity for FLASH’s unsplit PPM solver. The PPM approach (Colella & Woodward 1984) has been the most common hydrodynamics scheme used in simulating CCSNe (e.g., Fryxell et al. 1991; Janka & Mueller 1995; Rampp & Janka 2000; Blondin et al. 2003; Nordhaus et al. 2010; Couch 2013; Dolence et al. 2015; Lentz et al. 2015; Müller et al. 2012). The expected rates of convergence are recovered but we also see that at the same resolution, higher-order methods achieve substantially lower numerical viscosities, i.e., the magnitude of the truncation error of high-order schemes is smaller at equivalent resolution. The impact of this fact on computational efficiency can be profound. Say that for a given application it was decided that a numerical viscosity, in the units of Figure 2, no greater than 10^{-6} was required. Figure 2 implies that a third-order scheme such as PPM would require about *ten times* the resolution of the fifth-order WENO scheme. In 3D, this equates to an increase of 10,000 in computational expense!

Figure 2 also shows the post-bounce central density evolution from several 1D CCSN simulations at different grid resolutions comparing Spark-M1 using WENO5 to FLASH’s PPM solver. The effect of low resolution and excessive numerical viscosity would be to slow the contraction of the PNS. This is exactly what we find for coarser resolutions in Figure 2 but the comparison between WENO5 and PPM is striking. The impact of decreased resolution on PPM is much more dramatic and 1 km resolution PPM is no longer able to hold the PNS together and the central density actually *decreases* following core bounce. The difference between the central density evolution for WENO5 is far more subtle and WENO5 is able to keep the PNS together even at a grid resolution of 1 km.

Year 1 – Total Request: 150M Mira core-hours; 9M Theta core-hours

2.2 High-fidelity 3D MHD Simulations of CCSNe

In Year 1, we will carry out a set of high-resolution 3D CCSN simulations using Spark-M1 using progenitors that include realistic rotation rates and magnetic field strengths. We will construct our own 1D progenitor models using the open-source MESA code (Paxton et al. 2011, 2013, 2015) including rotational mixing instabilities and the Tayler-Spruit dynamo mechanism for magnetic field generation and angular mo-

mentum transport (Spruit 2002; Heger et al. 2005). Recent asteroseismology results for low-mass stars seem to indicate that the Tayler-Spruit mechanism may *underestimate* the amount of angular momentum transport out of rotating stellar cores (Cantiello et al. 2014). Thus, we will explore different coupling parameters in the stellar evolution models to construct cores of differing rotation rates for the same zero-age main sequence (ZAMS) masses. Using MESA, we will simulate a range of ZAMS masses and angular momentum transport parameters. From these models, we will select four to simulate in 3D using Spark-M1: “low” and “high” core rotation rates for a $\sim 10-M_{\odot}$ star and a $\sim 20-M_{\odot}$ star. The exact initial models used will be decided based on the results of a set of 2D simulations using Spark-M1 that will be completed prior to the start of Year 1. The initial magnetic field strengths for the 3D simulations will be taken directly from the values achieved in the 1D MESA models. The initial field geometry and spatial dependence will be a mix of poloidal and toroidal components guided by the 1D MESA models.

We will simulate in 3D these four models from the onset of core collapse through core bounce to ~ 500 ms post-bounce. Using AMR on a 3D Cartesian mesh, the maximum allowed refinement level will drop approximately logarithmically with radius from the center of the PNS. The highest level of refinement will achieve a resolution of 650 m and cover the inner ~ 80 km in radius, sufficient to keep the entire PNS and neutrinospheres at the same resolution. The second level of refinement at resolution of 1.3 km will reach out to 160 km in radius, sufficient to encompass the entire post-shock gain region until the onset of explosive shock expansion in most cases. This roughly equates to “angular” resolution varying between 0.47° and 0.93° . This is slightly coarser than the resolution we are using in the “high”-resolution 3D simulations of our current INCITE project but our results from those simulations do not show dramatic differences at this reduced resolution (see Section 1.1). Furthermore, our use of higher-order WENO5 for the MHD solver will mitigate this substantially and, likely, result in a *reduced* numerical viscosity as compared to slight higher resolution simulations using PPM (see Fig. 2). And this resolution is still substantially greater than the $\sim 2^{\circ}$ angular resolution used by other comparable high-fidelity 3D simulations of CCSNe (e.g., Nelson et al. 2015; Lentz et al. 2015; Janka et al. 2016). Each of the four 3D simulations will require 16M core-hours on *Mira* and 10 TB of online storage (see Section 3.3). Including 2M *Mira* core-hours for development and testing, the total request for this milestone is 66M *Mira* core-hours and 40 TB of online storage.

In addition to the simulations on *Mira*, in Year 1 we will execute two 3D CCSN simulations using Spark-M1 on *Theta*. Using a Director’s Discretionary allocation, we have already begun porting Spark-M1 to *Theta* (see Section 3). Without any machine-specific tuning, our Spark-M1 application shows a performance increase of *4-5x per thread* on *Theta* as compared to *Mira*. For these two simulations we will use the 10- and $20-M_{\odot}$ progenitors as above but without rotation or magnetic fields. These will serve as interesting and relevant control cases for this Y1 milestone while also being an excellent opportunity to adapt and tune Spark-M1 for *Theta*. One of the optimizations we plan for *Theta* is the implementation of a “marching cubes” approach for handling the large EOS and opacity tables. In this approach, each MPI rank will keep in memory only a reduced table covering the physical range in density, temperature, and electron fraction only of the zones owned by that rank, substantially reducing the memory footprint of these tables. For these two simulations we request a total of 8M *Theta* core-hours (26M *Mira*-equivalent core-hours) and 20 TB of online storage. Plus an additional 1M *Theta* core-hours for development and testing, the total request for *Theta* in Y1 is 9M core-hours (29.25M *Mira*-equivalent core-hours).

2.3 3D Simulations of Iron Core Collapse in Rotating Stars

One of the most remarkable and exciting results of recent 3D simulations of the CCSN mechanism is the discovery that realistic non-spherical structure in the progenitor star can have a dramatic impact (Couch & Ott 2013, 2015; Couch et al. 2015; Müller & Janka 2015; Müller et al. 2017). The breaking of spherical symmetry is manifest in the turbulent convection driven by nuclear burning in the cores of massive stars. As a massive star nears collapse, strongly convective burning in the Si and O shells surrounding the iron core can reach speeds of nearly 1000 km s⁻¹ and is characteristically very large in spatial scale (Arnett &

(Meakin 2011; Couch et al. 2015; Müller et al. 2016). These convective perturbations will reach the stalled shock shortly after core bounce and can aid neutrino-driven explosions by either enhancing the strength of post-shock turbulence (Couch & Ott 2015) or causing large scale “forced shock deformations” (Müller et al. 2017), or both. These results serve to remind us that CCSN mechanism simulations are initial value problems and that the details of our initial conditions matter tremendously! Our work inaugurated the era of detailed investigation into the impact of 3D progenitor structure on the CCSN mechanism (Couch & Ott 2013; Couch et al. 2015). As part of this INCITE project we will substantially expand the investigation into realistic progenitor structure for use in CCSN simulations.

We propose to carry out a series of new, high-fidelity 3D simulations of the final minutes of stellar evolution to the point of iron core collapse. As part of the pending SciDAC TEAMS collaboration, we are working with M. Zingale to adapt the Maestro low-mach number code (Almgren et al. 2007) to massive stellar cores. This will allow simulation of much longer time scales than currently possible (a few minutes; Couch et al. 2015; Müller et al. 2016). In the meantime, as part of this INCITE project we will continue the use of FLASH in simulating the minutes up to core collapse in 3D. For these simulations we will use the Spark MHD solver (Couch 2017) and include rotation and magnetic fields *for the first time ever* in a 3D CCSN progenitor simulation. Specifically, we will use the four 1D MESA progenitor models selected for 3D CCSN simulation in Section 2.2, initialized in 3D approximately five minutes prior to core collapse. We will follow the final build up of the iron core to its critical mass and ensuing collapse using an approximate 21-isotope nuclear network (Couch et al. 2015). We have recently made improvements to this network’s handling of weak interactions that bring the evolution into better agreement with the 1D evolution from the MESA code. We are currently simulating non-rotating, non-magnetic progenitors with this application in 2D and 3D.

Using AMR in Cartesian coordinates, we will use an approximate angular resolution of $\sim 0.5^\circ$, as in (Couch et al. 2015) and finer than that used by (Müller et al. 2017). Additionally, we will use Spark’s high-order WENO5 reconstruction to achieve much lower numerical viscosity than PPM at comparable resolution. Each such simulation will require 5M core-hours on *Mira*, for a total of 20M core-hours for the four simulations, plus 2M core-hours for development. We request 10 TB of online storage for these simulations. We will make the final 3D progenitor models publicly available and provide reader and interpolation routines in Fortran and Python for accessing the data so that other groups can readily incorporate these new 3D progenitors into their CCSN simulations. We will incorporate these first-of-their-kind 3D magnetorotational progenitor models into our CCSN mechanism simulations in Year 2 and 3 of this INCITE project.

2.4 High-resolution Simulation of Magnetorotational Turbulence in CCSNe

The neutrino-heated gain region in CCSNe is highly turbulent with physical Reynolds numbers $\sim 10^{17}$. Numerous recent works have pointed out that the larger numerical viscosities due to finite resolution in current 3D CCSN simulations is such that the effective *numerical* Reynolds numbers may only be a few hundred (Couch & Ott 2015; Abdikamalov et al. 2015; Radice et al. 2015, 2016), arguably not even turbulent. This could have a significant impact on the dynamics of the simulations, including a “bottleneck” effect preventing an efficient cascade of turbulent kinetic energy from large to small scales (Hanke et al. 2012; Couch 2013; Abdikamalov et al. 2015; Radice et al. 2016). Since the transition from stalled shock to explosion in 3D is attended by the appearance of the large-scale buoyant plumes behind the shock (Dolence et al. 2013; Müller et al. 2017), this bottleneck could have a crucial impact on the qualitative outcome of CCSN simulations.

The highest-resolution 3D CCSN simulations with high-fidelity neutrino transport have only used ~ 1 km resolution in the gain region (Roberts et al. 2016; O’Connor & Couch 2017). The parameterized simulations Radice et al. (2016) show that this resolution is not sufficient to correctly capture the turbulent cascade, though it is close to correctly calculating the turbulent kinetic energy on large scales. We propose to carry out the highest resolution neutrino-radiation hydrodynamic CCSN simulation yet. This simulation will have

critical value as a validation of the resolution used in current 3D CCSN simulations. For this simulation, we will allow the entire post-shock region to be refined up to a resolution of 650 m, twice the resolution of our fiducial model set (Section 2.2). Coupled with the higher-order WENO5 scheme we will use, this simulation should achieve the highest numerical Reynolds number of any 3D CCN simulation yet. We will study the gain region turbulence in this simulation and make a careful comparison to our fiducial models. We will select the initial based on the results of the simulations in Section 2.2. This simulation will comprise approximately 100 million computational zones. We will simulate approximately 500 ms of post-bounce evolution, bringing the request for this simulation to 62M core-hours and 40 TB of online storage.

Year 2 – Total Request: 150M *Mira* core-hours; 18M *Theta* core-hours

2.5 Late time 3D Simulations of Magnetorotational CCSNe

In Year 2 of this project will carry the 3D simulations of magnetorotational CCSNe of Section 2.2 to late times, at least one second post-bounce. Long time scale simulations are crucial for accurately predicting the explosion energy, PNS mass, nucleosynthesis, etc. (Bruenn et al. 2016; Müller et al. 2017). For any of the simulations that fail to explode, we will attempt to simulate late enough times to capture the onset of PNS collapse to a black hole. This has the potential to elucidate some details of the formation of stellar mass black holes, such as those that have been detected by aLIGO (Abbott et al. 2016, 2017). We have recently shown (Pan et al. 2017) that the GR effective potential approach can fairly accurately predict black hole formation time in 2D as compared to 1D fully GR simulations (O’Connor & Ott 2011).

The nucleosynthetic yields from CCSN simulations are a key quantity that can be directly compared to observations and laboratory measurements of cosmic abundances. We will compute the detailed nucleosynthesis from these late-time CCSN simulations. This will be accomplished as a post-processing step using the open-source SkyNet nuclear reaction network code developed by Co-I Roberts. The input for the nuclear reaction networks will be passive tracer particle data that records thermodynamic trajectory information from our FLASH CCSN simulations. FLASH already includes a well-developed, efficient passive-particle framework that has been used extensively in the calculation of nucleosynthesis in Type Ia supernova simulations (e.g., Long et al. 2014). We will compute detailed abundances for elements such as radioactive nickel and titanium, two key observable quantities, and we will also examine how rotation and magnetic fields can influence the conditions for very heavy element formation and the r-process.

Each of the four 3D simulations will require 16M core-hours on *Mira* and 10 TB of online storage (see Section 3.3). Including 2M *Mira* core-hours for development and testing, the total request for this milestone is 66M *Mira* core-hours and 40 TB of online storage.

2.6 3D Simulations of Iron Core Collapse in Rotating Stars

In Year 2, we will extend the Year 1 study of iron core collapse in rotating stars (Section 2.3 to more initial stellar masses. We will simulate the final five minutes of stellar evolution to core collapse in 3D for 15- and $25-M_{\odot}$ progenitor stars for both “high” and “low” core rotation rates. As in Year 1, all final models will be made publicly available. Each such simulation will require 5M core-hours on *Mira*, for a total of 20M core-hours for the four simulations. We request 10 TB of online storage for these simulations. We request an additional 2M core-hours for testing and development.

2.7 Capturing the Magnetorotational Instability and α - Ω Dynamo in the PNS

There is a very strong shear layer at the edge of rotating PNS’s that is unstable to the magnetorotational instability (MRI, Akiyama et al. 2003; Burrows et al. 2007). The presence of convection combined with rotation in the PNS can also lead to an α - Ω dynamo (Mösta et al. 2015). Both mechanisms can lead to exponential amplification of magnetic fields with dramatic implications for the CCSN mechanism. Accurately capturing either process is extremely challenging computationally, requiring extremely high resolution to capture the fastest growing modes of these instabilities (Mösta et al. 2015). In Year 2 of this project, we will

carry out an extremely high resolution simulation of a rotating PNS in order to study the rapid growth of magnetic fields via the MRI and dynamo. This simulation will go beyond Mösta et al. (2015) in a number of ways: we will use our M1 neutrino transport method rather than leakage, we will include the entire solid angle of the sphere rather than just a 90° wedge, and will simulate to later times in the aim of capturing the saturation of the magnetic fields. Using AMR, we will add two extra levels of refinement beyond our fiducial resolution (see Section 2.2) only in the shear layer surrounding the PNS, between 15 km and 40 km, bringing the finest resolution elements to 163 m. This approach was piloted for capturing turbulence in the gain region during our current INCITE project and will avoid adding additional zones in regions that are stable to the instabilities of interest. This is not as high as the highest resolution used by Mösta et al. (2015) but we plan to go to much longer time scales, as much as 100 ms post-bounce. This simulation will comprise about 100 million zones in 3D and require about 200,000 time steps to reach 100 ms. The expense for this simulation will be 60M core-hours on *Mira* and will require 40 TB of online storage. We request an additional 2M core-hours for testing and development.

2.8 MHD CCSN Simulations Using 3D Progenitors on *Theta*

In Year 2 we will use the 3D progenitor models generated in Year 1 (Sec. 2.3) for 3D MHD CCSN simulations on *Theta*. For these simulations, we will enhance the physical fidelity of our neutrino transport by incorporating the SciDAC TEAMS microphysics framework, if available. This planned open-source micro-physics framework will incorporate the latest, state of the art neutrino interactions and cross sections that are fully self-consistent with the underlying EOS.

For these four simulations we will use the 10- and 20- M_{\odot} 3D progenitors of Sec. 2.3. For this milestone we request a total of 16M *Theta* core-hours (52M *Mira*-equivalent core-hours) and 20 TB of online storage. Plus an additional 2M *Theta* core-hours for development and testing, the total request for *Theta* in Y2 is 18M core-hours (58.5M *Mira*-equivalent core-hours).

Year 3 – Total Request: 400M *Aurora* core-hours; 32M *Theta* core-hours

2.9 MHD CCSN Simulations Using 3D Progenitors

In Year 3 we will use the 3D progenitor models generated in Year 2 (Sec. 2.6) for 3D MHD CCSN simulations on *Theta*. For these four simulations we will use the 15- and 25- M_{\odot} 3D progenitors for both “high” and “low” rotation rates. For this milestone we request a total of 16M *Theta* core-hours (52M *Mira*-equivalent core-hours) and 40 TB of online storage.

2.10 Late time 3D Simulations of Magnetorotational CCSNe from 3D Progenitors

In Year 3 we will continue the four CCSN simulations in the 10- and 20- M_{\odot} progenitors to about one second post-bounce. As in Sec. 2.5, we will study the explosion energies, PNS masses, nucleosynthesis, and black hole formation times in these simulations as appropriate. For this milestone we request a total of 16M *Theta* core-hours (52M *Mira*-equivalent core-hours) and 40 TB of online storage.

2.11 Enhanced Physics CCSN Simulations in 3D Progenitors on *Aurora*

The advent of *Aurora* will be transformative for CCSN science. While many details remain to be worked out, *Aurora* will allow for larger parameter studies of high-fidelity, high-resolution, long-time scale 3D CCSN simulations. The potential to dramatically advance our understanding of stellar death is enormous. Conservatively assuming the same per-core performance as on *Theta*, a single 3D CCSN simulation to one second post-bounce will cost 8M core-hours on *Aurora*.

We propose to carry out a wide ranging study of the CCSN mechanism in a large number of realistic progenitor stars on *Aurora*. For these simulations, we will include inelastic neutrino scattering (O’Connor 2015; Burrows et al. 2016), and we estimate this will increase the simulation expense by at most 50%. Each simulation on *Aurora* will then cost 12M core-hours to reach one second. First, we will use the eight

fully 3D massive star progenitor models developed in Years 1 and 2 of this project. We will also simulate 12 additional initial stellar masses with two different rotation rates for a total of 24 additional 3D CCSN simulations. We will use MESA for constructing these initial models and will include rotation and magnetic fields in their evolution. In these simulations, since the progenitors themselves will be 1D, we will apply realistic perturbations to the velocity fields in the convective shells following either Müller & Janka (2015) or Chatzopoulos et al. (2014). For all 32 simulations, we request 384M core-hours on *Aurora*, plus 16M core-hours for development and testing. This milestone will require 2 PB of online storage. The specifics of these simulations may be altered based on the results of the work in Years 1 and 2.

3 Computational Readiness

3.1 Job Characterization & Use of Requested Resources

We estimate the computational cost of our simulations as follows. We assume an average shock radius of 200 km, inside of which the grid will be refined to the maximum allowed level. The maximum refinement level is radius dependent, establishing a grid in which the resolution increase logarithmically with radius. Given the rate of this decrease in refinement with radius, the average shock radius, and the finest possible grid spacing, dx_{\min} , the time-averaged number of zones, \bar{N}_{zones} , can be estimated for each simulation. Then, given the number of time steps needed, N_{steps} , the computational cost of a simulation is $C = \alpha \bar{N}_{\text{zones}} N_{\text{steps}}$, where α is the use rate in units of core-hours per zone-step. The number of time steps needed is determined by the evolution time sought and the time step size: $N_{\text{steps}} = t_{\max}/dt$. The time step for an explicit integrator is $dt = a_{\text{CFL}} \min[dx/(c_s + v)]$, where a_{CFL} is a number less than one (typically 0.5 for MHD and 0.9 for M1 transport), c_s is the maximum signal speed and v is the flow speed; this expression is computed locally for each zone. For *Spark-M1*, the explicit neutrino transport approach makes the maximum signal speed the speed of light, which is about three times the sound speed in the center of the PNS and, thus, is always the limiting signal speed (even though we use a larger a_{CFL} for the M1 update). The use rate, α , is determined experimentally from actual simulations (see §3.3). The time-averaged number of zones is estimated based on dx_{\min} , η , and the shock radius, behind which we assume maximal resolution. Comparison to actual production simulations shows that our method for estimating the the computational cost is accurate.

The vast majority of our requested allocation will be expended on jobs at the Capability scale (20% or more of the machine). We take two approaches to achieving this: large monolithic jobs and packaged smaller jobs. Specifically, the simulations proposed in Sections 2.2, 2.3, 2.5, and 2.6 will be packaged into 8192-node jobs on *Mira* wherein each individual simulation will run on a sub-partition of 2048 nodes. The simulations on *Theta* described in Sections 2.2, 2.8, 2.9, and 2.10 will also be packaged together into ensemble jobs, with individual jobs occupying \sim 150 nodes. The exact configuration will be decided based on extensive performance testing and tuning in Year 1. The large, high-fidelity parameter study planned for *Aurora* in Section 2.11 will also be packaged into multiple capability-scale ensemble jobs.

Data produced by our simulations will be retained on disk for analysis and post-processing for typically no longer than a year. Data will be automatically transferred to archival tape storage by our simulation management tool (see Section 3.2.1)

3.2 Computational Approach

Our primary tool for conducting the planned simulations will be the multi-physics, adaptive mesh refinement simulation framework, FLASH. Specifically, we will primarily use our custom CCSN application *Spark-M1* that incorporates the new, high-performance Spark MHD solver (Couch 2017) and our explicit two-moment neutrino transport solver (O'Connor 2015; O'Connor & Couch 2015). The code, now in its fourth major release version, has been continuously maintained, updated, extended, and modernized by the scientists at the Flash Center. Additionally, as an acceptance and Early Science application on BG/Q *Mira*, FLASH has been exacntly tuned to take advantage of this impressive architecture (see ?). The block-structured, oct-tree adaptive mesh refinement in FLASH provides extreme flexibility and efficiency,

particularly when combined with hybrid MPI/OpenMP parallelism. Coupled with the neutrino physics and nuclear equation of state that we have already implemented, FLASH is a code ideally suited to tackling the magnetorotational CCSN problem.

FLASH contains a wide range of numeric solvers for solving PDEs on block-structured AMR meshes. FLASH relies on the oct-tree based PARAMESH library (MacNeice et al. 2000). The proposed simulations will solve the equations of hydrodynamics and magnetohydrodynamics using an unsplit, explicit, finite-volume Eulerian formulation (see Sec. 2.1). FLASH utilizes hybrid MPI/OpenMP parallelism in order to make best use of many-core architectures. The hydrodynamics/MHD solvers, gravity solvers, and source terms have all been extended to include support for thread-level parallelism via OpenMP. FLASH writes output files using the HDF5 library. These files can be read in directly and visualized in parallel using VisIt or yt visualization software (Turk et al. 2011).

Our Spark-M1 application has been architected for performance. Options such as reconstruction and Riemann solver are selected at compilation rather than runtime and are generally directly in-lined into the calling routines in order to avoid function call overhead. Aggressive use of Fortran array operations are employed and facilitate easy vectorization by the compiler. In order to minimize cache misses, the reconstruction and flux calculation steps in Spark take place on auxiliary 1D “pencil” arrays that flatten an entire 1D ray of zones into a data structure that is contiguous in memory and much smaller than a one entire AMR block data structure. All 1D reconstruction and flux computations are completed on these rays then before moving on to other rays, maximizing the number of operations performed per byte of data moved from memory. This approach also facilitates efficient OpenMP threading wherein each thread operates on a collection of pencil arrays. Communication is avoided during the multi-stage RK integration by filling and updating extra layers of guard, or halo, zones. Thus, for WENO5, with a five-point stencil, and RK2 we require six guard zones per direction. The M1 neutrino transport equations form a hyperbolic system of PDEs that is extremely similar to the MHD equations in structure and, thus, can be solved with similar methods. Our implementation is a finite volume approach using second-order spatial reconstruction and third-order SSP RK time integration. This approach makes full use of all six guard zones per direction and the high-order time integration

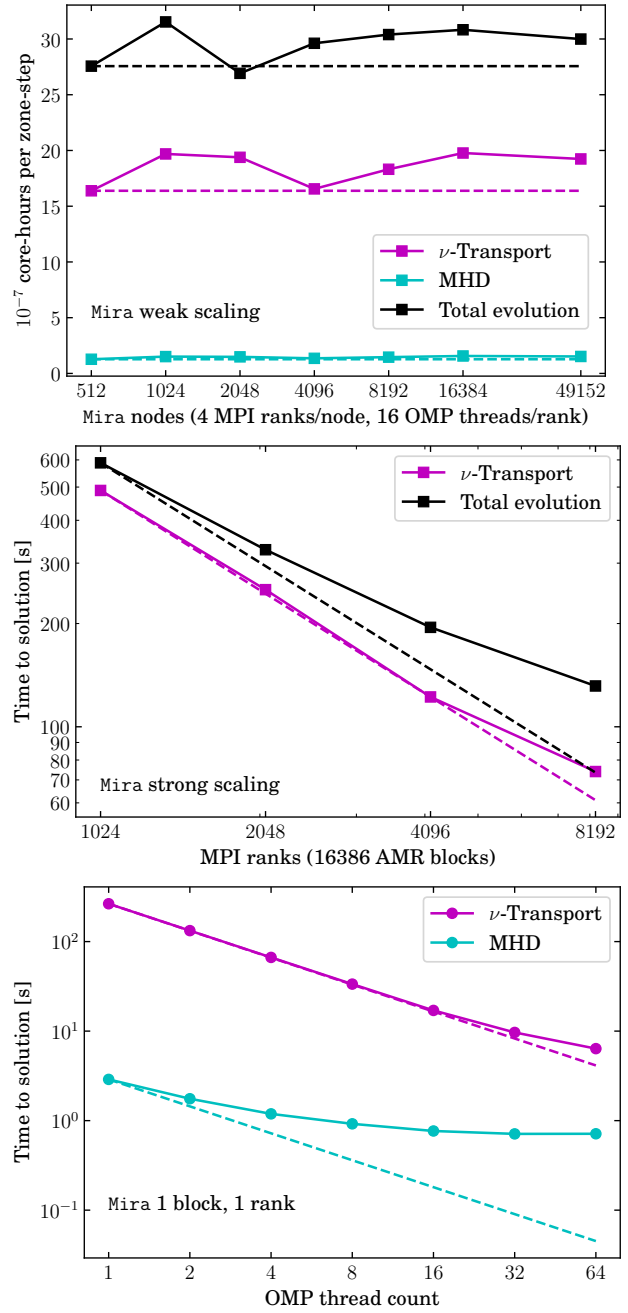


Figure 3: Weak scaling (top), strong scaling (middle), and threading speedup (bottom) of Spark-M1 on *Mira*.

hyperbolic system of PDEs that is extremely similar to the MHD equations in structure and, thus, can be solved with similar methods. Our implementation is a finite volume approach using second-order spatial reconstruction and third-order SSP RK time integration. This approach makes full use of all six guard zones per direction and the high-order time integration

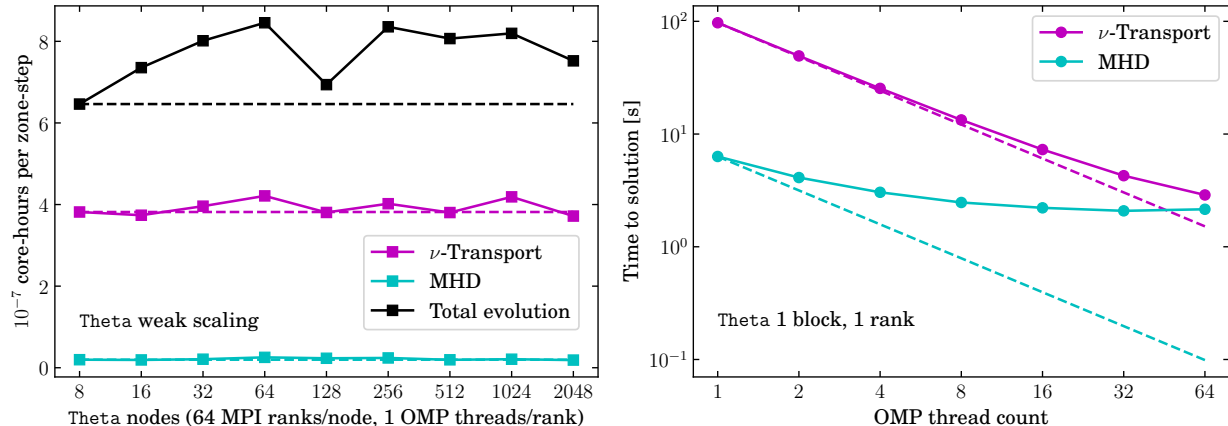


Figure 4: Weak scaling (left) and OpenMP thread-to-thread speedup for our Spark-M1 CCSN application on *Theta*.

increases stability, allowing M1-limited time steps up to CFL factors of $\gtrsim 0.9$, greater than the typical MHD-limited CFL factor of ~ 0.5 . This mitigates to some extent the increased number of time steps required by the explicit radiation transport approach and reduces the ratio of communication-to-computation.

3.2.1 Workflow Patterns

Our proposed research plan involves a multitude of simulations almost of all of which require several restarts and extensive post-processing visualization and analysis. In the past, we have used the Simulation management and analysis system (Smaash) that was custom-built for FLASH simulations. We found Smaash to have some nice features, but to suffer from portability and stability and have since resorted to shell scripts for automatically configuring and queuing restart jobs. This approach is robust and portable, but lacks any degree of in-flight monitoring, analysis, or visualization and is generally still very “hands-on.” We are currently developing a new simulation management tool in Python that seeks to retain the simplicity and portability of our shell scripts while being more full-featured. This management tool, SIMpliPy, will monitor simulation progress and perform simple runtime analysis and visualization using yt (Turk et al. 2011). SIMpliPy will also configure and schedule job restarts, handle job dependencies, and manage automatic transferal of simulation data to archival storage. SIMpliPy is borrowing ideas and features from the sumatra tool³ to enhance reproducibility of simulations and data provenance. SIMpliPy will primarily use standard Python features and libraries (such as JSON for metadata management) and git for version tracking in order to both speed development and provide portability.

3.2.2 I/O

Flash implements parallel HDF5 and collective I/O wherein a reduced number of MPI ranks perform I/O to reduce the number of processes accessing the file system at one time. The amount of time spent by FLASH on I/O in a production simulation is typically less than 10% of the overall run time.

3.3 Parallel Performance

We have benchmarked the performance and scaling of our Spark-M1 application on *Mira*, *Theta*, as well as commodity computers using recent Intel processors. Our scaling studies use the full, production version of Spark-M1, including MHD, self-gravity, AMR, M1 neutrino transport, and tabular equation of state. In Figure 3 we show the weak scaling on *Mira* for Spark-M1 going up to the entire machine, 49,152 nodes (786k cores). Weak scaling is essentially perfect, with an efficiency of 92% at 48,152 nodes as compared to 512 nodes, with some scatter as these tests represent realistic production-grade problem setups. This result

³<https://pythonhosted.org/Sumatra/>

Table 1. Single-thread performance comparisons on different hardware platforms in units of core-hours/zone-step (zone-step/core-second).

	FieldLoop Spark	FieldLoop USM-CT	CCSN Spark-M1	Progen Spark-Ap21
Intel Core i7 (I7-6567U)	2.15e-09 (129,075)	7.09e-09 (39,173)	1.80e-07 (1545)	4.30e-09 (64,378)
Intel Xeon E5-2680v4	1.76e-09 (157,808)	4.42e-09 (62,779)	1.05e-07 (2658)	3.52e-09 (78,904)
IBM BG/Q A2	2.58e-08 (10,787)	6.58e-08 (4221)	2.75e-06 (103)	5.16e-08 (5393)
Intel KNL	7.41e-09 (37,494)	2.81e-08 (9881)	7.00e-07 (397)	1.48e-08 (18,747)

is a dramatic improvement in weak scaling efficiency for our M1 neutrino transport application as compared to our INCTE proposal in 2014. We also plot in Fig. 3 the strong scaling and thread-to-thread speedup for Spark–M1. Our production simulations as planned will typically have four or more AMR blocks per MPI rank, putting them not near to the ideal strong scaling curve. OpenMP thread speed up is near-perfect for the M1 solver, although cache contention at more than 16 threads per rank becomes an issue). Threading efficiency could be improved for our MHD solver, but it typically represents a small fraction of overall runtime for our planned simulations and so is not a limiting factor.

We have also carried out an initial performance study of our Spark–M1 application on *Theta*. Figure 4 shows the weak scaling and threading speedup on *Theta*. Both are acceptable for our planned production simulations on *Theta*, but we stress that this is only on initial performance study as we have not yet done any performance tuning of Spark–M1 on *Theta*, only ported our application directly from *Mira*. Thus, we expect to realize substantial improvements in performance on *Theta* although we are already seeing an increase in per-core performance of 4x over *Mira* for Spark–M1! This is better even than the nominal increase in per-core FLOP rate between these two machines (3.25x).

In order to gauge the absolute performance of our new Spark MHD solver, we have benchmarked Spark against FLASH’s unsplit staggered-mesh constrained transport solver (USM-CT). We use the common Field Loop Advection problem described in [Gardiner & Stone \(2005\)](#) and [Lee et al. \(2009\)](#), which is a standard test problem packaged with the release versions of both codes. We have executed this benchmark on four different hardware platforms: a commodity laptop with a Intel Core i7 6567U processor, a Lenovo cluster with Intel Xeon E5-2680v4 processors, BG/Q Cetus with IBM A2 processors, and *Theta* with Intel Phi-Knights Hill chips. We use a fixed-resolution grid for these tests and the same parameters on all platforms using a single thread of execution.

The results of this benchmarking are shown in Table 1. On all platforms, Spark outperforms the USM-CT solver by a factor of \sim 3-4. Table 1 also shows the single-thread performance for our Spark–M1 CCSN application on these hardware platforms. Most notable is the increase in performance between BG/Q and Intel KNL. Without yet having done *any* machine-specific tuning for *Theta*, we find an increase in single-thread performance of \sim 4x over IBM BG/Q. The numbers for Spark–M1 in this table are used in making the required resource estimates throughout this proposal.

3.4 Developmental Work

Our Spark–M1 application is production ready for the simulations we plan for Year 1 of this project. During Year 1, we will profile and tune Spark–M1 on *Theta*. We also plan to implement a “marching cubes” scheme for storing EOS and opacity data. In this approach, only the portion of the very large (\sim 400 MB each) tables that is needed by a given MPI rank will be stored in that rank’s memory. Ideally, this would make the EOS and opacity data fit within the outer-most level of cache enabling substantial increase in performance. On *Theta*, this approach will ensure that the entire application easily fits within the high-bandwidth memory. One of the project postdocs, Kuo-Chuan Pan, is attending the Argonne Training

Program in Extreme-Scale Computing and will focus on tuning our application for *Theta*.

Much of the remainder of our development plans are targeted toward next-generation systems such as *Aurora* (see following section).

3.5 Development plan for next-generation systems

We will implement very high-order cell-centered constrained transport finite difference MHD methods (Christlieb et al. 2014, 2016). Using the method of differential transforms (Norman & Finkel 2012; Norman 2013; Seal et al. 2014), we will achieve not only high spatial order but high temporal order as well while maintaining a very compact spatial stencil, thus limiting the need for large numbers of ghost zones and attendant (expensive) inter-node communication. For example, a ninth-order WENO method using the method of differential transforms requires only eleven ghost zones per dimension to achieve ninth-order temporal accuracy (Seal et al. 2014). Additionally, we explore implementing order-adaptivity such that the spatial and temporal orders will be decreased in, e.g., shocks where high-order finite difference is undesirable.

We will also overhaul the main driver routines in `FLASH` to incorporate some limited task-based parallelism and one-sided MPI communication. For the former, we will use the unique `FLASH` build system to define `TASKS` and respective `DEPENDENCIES`. Physics solvers such as MHD are stencil based and thus have some dependence on neighboring data requiring that these operations wait until the ghost zone data are received from neighboring processes. Other solvers, such as nuclear burning and other local source terms, are not stencil based and so can be completed before ghost zone data are received. By restructuring the top-level driver routine in `FLASH`, we will exploit these differences in dependencies to increase the parallel efficiency of the application using a very limited form of task-based parallelism. This approach can even be extended to stencil-based operators such as MHD by taking advantage of the fact that the stencils used are typically much smaller than the linear size of the domain blocks, the fundamental units of parallelism in `FLASH`. Thus the domain blocks can be further sub-divided into completely node-local “tiles.” Some tiles will not have stencils that extend into any ghost zone regions and can therefore be computed before waiting for ghost zone communication to complete. Other tiles will depend on ghost zone data from a subset of the neighboring processes and can then be worked on once communication is completed with only those processes.

We also plan to overhaul the ghost zone communication in `FLASH` by incorporating one-sided MPI communication through the use of user buffers for storing messages. These buffers may be in the NVRAM or the DDR4, while the memory needed by the task currently being executed will sit in the HBM.

We will also explore the possibility of implementing a novel data compression algorithm for time-series physics simulation data. For physics simulations that include small scale features that are *not* volume-filling, the full domain data does not need to be written to disk as frequently as regions that contain features of interest. This presents the opportunity for dramatic data compression through implementing an I/O scheme that adaptively selects subsets of the full domain data to write to disk frequently. For post-processing analysis and visualization could then be achieved by using image reconstruction methods to recover the coarsely sampled data at the desired sampling frequency. Machine learning methods could be employed to intelligently save data at the correct sampling rate to retain a specified level of accuracy in the reconstructed data. We will engage the ExaHDF5 group in the feasibility of implementing such an I/O scheme.

Our approach for portability in this project will be to continue `FLASH`’s reliance principally on MPI and HDF5 while incorporating the emerging OpenMP 4.x standard for on-node thread parallelism. OpenMP 4.x implements unified directives for both many-core chips such as Intel Phi and for GPGPU accelerators. The physics solvers in `FLASH` are already threaded using OpenMP so the extension to the new 4.x standard will be relatively straightforward.

References

- Abbott, B. P., Abbott, R., Abbott, T. D., Abernathy, M. R., Acernese, F., Ackley, K., Adams, C., Adams, T., Addesso, P., Adhikari, R. X., et al., 2016, *Observation of Gravitational Waves from a Binary Black Hole Merger*, *Physical Review Letters*, 116, 061102
- Abbott, B. P., Abbott, R., Abbott, T. D., Acernese, F., Ackley, K., Adams, C., Adams, T., Addesso, P., Adhikari, R. X., Adya, V. B., et al., 2017, *GW170104: Observation of a 50-Solar-Mass Binary Black Hole Coalescence at Redshift 0.2*, *Physical Review Letters*, 118, 221101
- Abdikamalov, E., Ott, C. D., Radice, D., Roberts, L. F., Haas, R., Reisswig, C., Mösta, P., Klion, H., Schnetter, E., 2015, *Neutrino-driven Turbulent Convection and Standing Accretion Shock Instability in Three-dimensional Core-collapse Supernovae*, *ApJ*, 808, 70
- Akiyama, S., Wheeler, J. C., Meier, D. L., Lichtenstadt, I., 2003, *The Magnetorotational Instability in Core-Collapse Supernova Explosions*, *ApJ*, 584, 954-970
- Almgren, A. S., Beckner, V. E., Bell, J. B., Day, M. S., Howell, L. H., Joggerst, C. C., Lijewski, M. J., Nonaka, A., Singer, M., Zingale, M., 2010, *CASTRO: A New Compressible Astrophysical Solver. I. Hydrodynamics and Self-gravity*, *ApJ*, 715, 1221-1238
- Almgren, A. S., Bell, J. B., Zingale, M., 2007, *MAESTRO: A Low Mach Number Stellar Hydrodynamics Code*, *Journal of Physics Conference Series*, 78, 012085
- Arnett, W. D., Meakin, C., 2011, *Toward Realistic Progenitors of Core-collapse Supernovae*, *ApJ*, 733, 78
- Balbus, S. A., Hawley, J. F., 1991, *A powerful local shear instability in weakly magnetized disks. I - Linear analysis. II - Nonlinear evolution*, *ApJ*, 376, 214-233
- Blondin, J. M., Mezzacappa, A., DeMarino, C., 2003, *Stability of Standing Accretion Shocks, with an Eye toward Core-Collapse Supernovae*, *ApJ*, 584, 971-980
- Borges, R., Carmona, M., Costa, B., Don, W. S., 2008, *An improved weighted essentially non-oscillatory scheme for hyperbolic conservation laws*, *Journal of Computational Physics*, 227, 3191-3211
- Bruenn, S. W., Lentz, E. J., Hix, W. R., Mezzacappa, A., Harris, J. A., Messer, O. E. B., Endeve, E., Blondin, J. M., Chertkow, M. A., Lingerfelt, E. J., Marronetti, P., Yakunin, K. N., 2016, *The Development of Explosions in Axisymmetric Ab Initio Core-collapse Supernova Simulations of 12-25 M Stars*, *ApJ*, 818, 123
- Bruenn, S. W., Mezzacappa, A., Hix, W. R., Lentz, E. J., Messer, O. E. B., Lingerfelt, E. J., Blondin, J. M., Endeve, E., Marronetti, P., Yakunin, K. N., 2013, *Axisymmetric Ab Initio Core-collapse Supernova Simulations of 12-25 M_⊙ Stars*, *ApJ*, 767, L6
- Burrows, A., Dessart, L., Livne, E., Ott, C. D., Murphy, J., 2007, *Simulations of Magnetically Driven Supernova and Hypernova Explosions in the Context of Rapid Rotation*, *ApJ*, 664, 416-434
- Burrows, A., Hayes, J., 1996, *Pulsar Recoil and Gravitational Radiation Due to Asymmetrical Stellar Collapse and Explosion*, *Physical Review Letters*, 76, 352-355
- Burrows, A., Vartanyan, D., Dolence, J. C., Skinner, M. A., Radice, D., 2016, *Crucial Physical Dependencies of the Core-Collapse Supernova Mechanism*, *ArXiv e-prints*
- Cantiello, M., Mankovich, C., Bildsten, L., Christensen-Dalsgaard, J., Paxton, B., 2014, *Angular Momentum Transport within Evolved Low-mass Stars*, *ApJ*, 788, 93
- Chandrasekhar, S., 1961, *Hydrodynamic and hydromagnetic stability*
- Chatzopoulos, E., Graziani, C., Couch, S. M., 2014, *Characterizing the Convective Velocity Fields in Massive Stars*, *ApJ*, 795, 92
- Christlieb, A. J., Feng, X., Seal, D. C., Tang, Q., 2016, *A high-order positivity-preserving single-stage single-step method for the ideal magnetohydrodynamic equations*, *Journal of Computational Physics*, 316, 218-242

- Christlieb, A. J., Rossmanith, J. A., Tang, Q., 2014, *Finite difference weighted essentially non-oscillatory schemes with constrained transport for ideal magnetohydrodynamics*, *Journal of Computational Physics*, 268, 302-325
- Colella, P., Glaz, H. M., 1985, *Efficient solution algorithms for the Riemann problem for real gases*, *Journal of Computational Physics*, 59, 264-289
- Colella, P., Woodward, P. R., 1984, *The Piecewise Parabolic Method (PPM) for Gas-Dynamical Simulations*, *Journal of Computational Physics*, 54, 174-201
- Colgate, S. A., Grasberger, W. H., White, R. H., 1961, *The Dynamics of Supernova Explosions*, *AJ*, 66, 280
- Couch, S. M., 2013, *On the Impact of Three Dimensions in Simulations of Neutrino-driven Core-collapse Supernova Explosions*, *ApJ*, 775, 35
- , 2017, *Spark: A New Solver for Self-gravitating Compressible Magnetohydrodynamics Implemented in the FLASH Simulation Framework*, *in prep.*
- Couch, S. M., Chatzopoulos, E., Arnett, W. D., Timmes, F. X., 2015, *The Three-dimensional Evolution to Core Collapse of a Massive Star*, *ApJ*, 808, L21
- Couch, S. M., Graziani, C., Flocke, N., 2013, *An Improved Multipole Approximation for Self-gravity and Its Importance for Core-collapse Supernova Simulations*, *ApJ*, 778, 181
- Couch, S. M., Ott, C. D., 2013, *Revival of the Stalled Core-collapse Supernova Shock Triggered by Precollapse Asphericity in the Progenitor Star*, *ApJ*, 778, L7
- , 2015, *The Role of Turbulence in Neutrino-driven Core-collapse Supernova Explosions*, *ApJ*, 799, 5
- Dedner, A., Kemm, F., Kröner, D., Munz, C.-D., Schnitzer, T., Wesenberg, M., 2002, *Hyperbolic Divergence Cleaning for the MHD Equations*, *Journal of Computational Physics*, 175, 645-673
- Dolence, J. C., Burrows, A., Murphy, J. W., Nordhaus, J., 2013, *Dimensional Dependence of the Hydrodynamics of Core-collapse Supernovae*, *ApJ*, 765, 110
- Dolence, J. C., Burrows, A., Zhang, W., 2015, *Two-dimensional Core-collapse Supernova Models with Multi-dimensional Transport*, *ApJ*, 800, 10
- Dubey, A., Reid, L. B., Weide, K., Antypas, K., Ganapathy, M. K., Riley, K., Sheeler, D., Siegal, A., 2009, *Extensible Component Based Architecture for FLASH, A Massively Parallel, Multiphysics Simulation Code*, *Parallel Computing*, 35, 512-522
- Fryxell, B., Arnett, D., Mueller, E., 1991, *Instabilities and clumping in SN 1987A. I - Early evolution in two dimensions*, *ApJ*, 367, 619-634
- Fryxell, B., Olson, K., Ricker, P., Timmes, F. X., Zingale, M., Lamb, D. Q., MacNeice, P., Rosner, R., Truran, J. W., Tufo, H., 2000, *FLASH: An Adaptive Mesh Hydrodynamics Code for Modeling Astrophysical Thermonuclear Flashes*, *ApJS*, 131, 273-334
- Gardiner, T. A., Stone, J. M., 2005, *An unsplit Godunov method for ideal MHD via constrained transport*, *Journal of Computational Physics*, 205, 509-539
- Gottlieb, S., Shu, C. W., 1998, *Total variation diminishing Runge-Kutta schemes*, *Mathematics of Computation*, 67, 73-85
- Hanke, F., Marek, A., Müller, B., Janka, H.-T., 2012, *Is Strong SASI Activity the Key to Successful Neutrino-driven Supernova Explosions?*, *ApJ*, 755, 138
- Hanke, F., Müller, B., Wongwathanarat, A., Marek, A., Janka, H.-T., 2013, *SASI Activity in Three-dimensional Neutrino-hydrodynamics Simulations of Supernova Cores*, *ApJ*, 770, 66
- Heger, A., Woosley, S. E., Spruit, H. C., 2005, *Presupernova Evolution of Differentially Rotating Massive Stars Including Magnetic Fields*, *ApJ*, 626, 350-363
- Janka, H.-T., Melson, T., Summa, A., 2016, *Physics of Core-Collapse Supernovae in Three Dimensions: A*

- Sneak Preview, Annual Review of Nuclear and Particle Science*, 66, 341-375
- Janka, H.-T., Mueller, E., 1995, *The First Second of a Type II Supernova: Convection, Accretion, and Shock Propagation*, *ApJ*, 448, L109
- Jiang, G.-S., Wu, C.-c., 1999, *A High-Order WENO Finite Difference Scheme for the Equations of Ideal Magnetohydrodynamics*, *Journal of Computational Physics*, 150, 561-594
- Just, O., Obergaulinger, M., Janka, H.-T., 2015, *A new multidimensional, energy-dependent two-moment transport code for neutrino-hydrodynamics*, *MNRAS*, 453, 3386-3413
- Kuroda, T., Takiwaki, T., Kotake, K., 2016, *A New Multi-energy Neutrino Radiation-Hydrodynamics Code in Full General Relativity and Its Application to the Gravitational Collapse of Massive Stars*, *ApJS*, 222, 20
- LeBlanc, J. M., Wilson, J. R., 1970, *A Numerical Example of the Collapse of a Rotating Magnetized Star*, *ApJ*, 161, 541
- Lee, D., 2013, *A solution accurate, efficient and stable unsplit staggered mesh scheme for three dimensional magnetohydrodynamics*, *Journal of Computational Physics*, 243, 269-292
- Lee, D., Deane, A. E., 2009, *An unsplit staggered mesh scheme for multidimensional magnetohydrodynamics*, *Journal of Computational Physics*, 228, 952-975
- Lee, W. H., Ramirez-Ruiz, E., López-Cámarra, D., 2009, *Phase Transitions and He-Synthesis-Driven Winds in Neutrino Cooled Accretion Disks: Prospects for Late Flares in Short Gamma-Ray Bursts*, *ApJ*, 699, L93-L96
- Lentz, E. J., Bruenn, S. W., Hix, W. R., Mezzacappa, A., Messer, O. E. B., Endeve, E., Blondin, J. M., Harris, J. A., Marronetti, P., Yakunin, K. N., 2015, *Three-dimensional Core-collapse Supernova Simulated Using a $15 M_{\odot}$ Progenitor*, *ApJ*, 807, L31
- Long, M., Jordan IV, G. C., van Rossum, D. R., Diemer, B., Graziani, C., Kessler, R., Meyer, B., Rich, P., Lamb, D. Q., 2014, *Three-dimensional Simulations of Pure Deflagration Models for Thermonuclear Supernovae*, *ApJ*, 789, 103
- MacNeice, P., Olson, K. M., Mobarry, C., de Fainchtein, R., Packer, C., 2000, *PARAMESH: A parallel adaptive mesh refinement community toolkit*, *Computer Physics Communications*, 126, 330-354
- Marek, A., Dimmelmeier, H., Janka, H.-T., Müller, E., Buras, R., 2006, *Exploring the relativistic regime with Newtonian hydrodynamics: an improved effective gravitational potential for supernova simulations*, *A&A*, 445, 273-289
- Meakin, C. A., Arnett, D., 2007, *Turbulent Convection in Stellar Interiors. I. Hydrodynamic Simulation*, *ApJ*, 667, 448-475
- Melson, T., Janka, H.-T., Bollig, R., Hanke, F., Marek, A., Müller, B., 2015, *Neutrino-driven Explosion of a 20 Solar-mass Star in Three Dimensions Enabled by Strange-quark Contributions to Neutrino-Nucleon Scattering*, *ApJ*, 808, L42
- Mignone, A., Tzeferacos, P., Bodo, G., 2010, *High-order conservative finite difference GLM-MHD schemes for cell-centered MHD*, *Journal of Computational Physics*, 229, 5896-5920
- Miyoshi, T., Kusano, K., 2005, *A multi-state HLL approximate Riemann solver for ideal magnetohydrodynamics*, *Journal of Computational Physics*, 208, 315-344
- Modjaz, M., Liu, Y. Q., Bianco, F. B., Graur, O., 2016, *The Spectral SN-GRB Connection: Systematic Spectral Comparisons between Type Ic Supernovae and Broad-lined Type Ic Supernovae with and without Gamma-Ray Bursts*, *ApJ*, 832, 108
- Mösta, P., Ott, C. D., Radice, D., Roberts, L. F., Schnetter, E., Haas, R., 2015, *A large-scale dynamo and magnetoturbulence in rapidly rotating core-collapse supernovae*, *Nature*, 528, 376-379
- Müller, B., Janka, H.-T., 2015, *Non-radial instabilities and progenitor asphericities in core-collapse super-*

- novae, MNRAS, 448, 2141-2174*
- Müller, B., Janka, H.-T., Marek, A., 2012, *A New Multi-dimensional General Relativistic Neutrino Hydrodynamics Code for Core-collapse Supernovae. II. Relativistic Explosion Models of Core-collapse Supernovae, ApJ, 756, 84*
- Müller, B., Melson, T., Heger, A., Janka, H.-T., 2017, *Supernova Simulations from a 3D Progenitor Model – Impact of Perturbations and Evolution of Explosion Properties, ArXiv e-prints*
- Müller, B., Viallet, M., Heger, A., Janka, H.-T., 2016, *The Last Minutes of Oxygen Shell Burning in a Massive Star, ApJ, 833, 124*
- Murchikova, L., Abdikamalov, E., Urbatsch, T., 2017, *Analytic Closures for M1 Neutrino Transport, ArXiv e-prints*
- Murphy, J. W., Dolence, J. C., Burrows, A., 2013, *The Dominance of Neutrino-driven Convection in Core-collapse Supernovae, ApJ, 771, 52*
- Nordhaus, J., Burrows, A., Almgren, A., Bell, J., 2010, *Dimension as a Key to the Neutrino Mechanism of Core-collapse Supernova Explosions, ApJ, 720, 694-703*
- Norman, M. R., 2013, *Algorithmic improvements for schemes using the ADER time discretization, Journal of Computational Physics, 243, 176-178*
- Norman, M. R., Finkel, H., 2012, *Multi-moment ADER-Taylor methods for systems of conservation laws with source terms in one dimension, Journal of Computational Physics, 231, 6622-6642*
- Obergaulinger, M., Cerdá-Durán, P., Müller, E., Aloy, M. A., 2009, *Semi-global simulations of the magneto-rotational instability in core collapse supernovae, A&A, 498, 241-271*
- O'Connor, E., 2015, *An Open-source Neutrino Radiation Hydrodynamics Code for Core-collapse Supernovae, ApJS, 219, 24*
- O'Connor, E., Couch, S. M., 2015, *Core-collapse Supernova Simulations with Multidimensional Two-moment Neutrino Transport: Explosions Aided by General Relativity, submitted to ApJ*
- , 2017, *Three-dimensional Simulations of Core-collapse Supernovae with Multidimensional Neutrino Transport, in prep.*
- O'Connor, E., Horowitz, C. J., Lin, Z., Couch, S. M., 2017, *Core-Collapse Supernova Simulations including Neutrino Interactions from the Virial EOS, Proceeding of the International Astronomical Union Symposium: SN 1987A, 30 years later*
- O'Connor, E., Ott, C. D., 2010, *A new open-source code for spherically symmetric stellar collapse to neutron stars and black holes, Classical and Quantum Gravity, 27, 114103*
- , 2011, *Black Hole Formation in Failing Core-Collapse Supernovae, ApJ, 730, 70*
- , 2013, *The Progenitor Dependence of the Pre-explosion Neutrino Emission in Core-collapse Supernovae, ApJ, 762, 126*
- Ott, C. D., Burrows, A., Dessart, L., Livne, E., 2008, *Two-Dimensional Multiangle, Multigroup Neutrino Radiation-Hydrodynamic Simulations of Postbounce Supernova Cores, ApJ, 685, 1069-1088*
- Ott, C. D., Burrows, A., Thompson, T. A., Livne, E., Walder, R., 2006, *The Spin Periods and Rotational Profiles of Neutron Stars at Birth, ApJS, 164, 130-155*
- Pan, K.-C., Liebendorfer, M., Couch, S. M., Thielemann, F., 2017, *Impact of equations of state on black hole formation dynamics and gravitational wave signals from collapsar, in prep.*
- Paxton, B., Bildsten, L., Dotter, A., Herwig, F., Lesaffre, P., Timmes, F., 2011, *Modules for Experiments in Stellar Astrophysics (MESA), ApJS, 192, 3*
- Paxton, B., Cantiello, M., Arras, P., Bildsten, L., Brown, E. F., Dotter, A., Mankovich, C., Montgomery, M. H., Stello, D., Timmes, F. X., Townsend, R., 2013, *Modules for Experiments in Stellar Astrophysics*

- (MESA): *Planets, Oscillations, Rotation, and Massive Stars*, *ApJS*, 208, 4
- Paxton, B., Marchant, P., Schwab, J., Bauer, E. B., Bildsten, L., Cantiello, M., Dessart, L., Farmer, R., Hu, H., Langer, N., Townsend, R. H. D., Townsley, D. M., Timmes, F. X., 2015, *Modules for Experiments in Stellar Astrophysics (MESA): Binaries, Pulsations, and Explosions*, *ApJS*, 220, 15
- Pope, S. B., 2000, *Turbulent Flows*. p. 806
- Radice, D., Couch, S. M., Ott, C. D., 2015, *Implicit large eddy simulations of anisotropic weakly compressible turbulence with application to core-collapse supernovae*, *Computational Astrophysics and Cosmology*, 2, 7
- Radice, D., Ott, C. D., Abdikamalov, E., Couch, S. M., Haas, R., Schnetter, E., 2016, *Neutrino-driven Convection in Core-collapse Supernovae: High-resolution Simulations*, *ApJ*, 820, 76
- Rampp, M., Janka, H.-T., 2000, *Spherically Symmetric Simulation with Boltzmann Neutrino Transport of Core Collapse and Postbounce Evolution of a 15 M_{solar} Star*, *ApJ*, 539, L33-L36
- Rembiasz, T., Obergaulinger, M., Cerdá-Durán, P., Aloy, M.-Á., Müller, E., 2016, *On the measurements of numerical viscosity and resistivity in Eulerian MHD codes*, *ArXiv e-prints*
- Roberts, L. F., Ott, C. D., Haas, R., O'Connor, E. P., Diener, P., Schnetter, E., 2016, *General-Relativistic Three-Dimensional Multi-group Neutrino Radiation-Hydrodynamics Simulations of Core-Collapse Supernovae*, *ApJ*, 831, 98
- Seal, D. C., Güclü, Y., Christlieb, A. J., 2014, *The Picard integral formulation of weighted essentially non-oscillatory schemes*, *ArXiv e-prints*
- Shibata, M., Kiuchi, K., Sekiguchi, Y., Suwa, Y., 2011, *Truncated Moment Formalism for Radiation Hydrodynamics in Numerical Relativity*, *Progress of Theoretical Physics*, 125, 1255-1287
- Skinner, M. A., Burrows, A., Dolence, J. C., 2016, *Should One Use the Ray-by-Ray Approximation in Core-collapse Supernova Simulations?*, *ApJ*, 831, 81
- Spruit, H. C., 2002, *Dynamo action by differential rotation in a stably stratified stellar interior*, *A&A*, 381, 923-932
- Thompson, T. A., Quataert, E., Burrows, A., 2005, *Viscosity and Rotation in Core-Collapse Supernovae*, *ApJ*, 620, 861-877
- Turk, M. J., Smith, B. D., Oishi, J. S., Skory, S., Skillman, S. W., Abel, T., Norman, M. L., 2011, *yt: A Multi-code Analysis Toolkit for Astrophysical Simulation Data*, *ApJS*, 192, 9
- Wheeler, J. C., Meier, D. L., Wilson, J. R., 2002, *Asymmetric Supernovae from Magnetocentrifugal Jets*, *ApJ*, 568, 807-819
- Wheeler, J. C., Yi, I., Höflich, P., Wang, L., 2000, *Asymmetric Supernovae, Pulsars, Magnetars, and Gamma-Ray Bursts*, *ApJ*, 537, 810-823
- Winteler, C., Käppeli, R., Perego, A., Arcones, A., Vasset, N., Nishimura, N., Liebendörfer, M., Thielemann, F.-K., 2012, *Magnetorotationally Driven Supernovae as the Origin of Early Galaxy r-process Elements?*, *ApJ*, 750, L22
- Woosley, S. E., Heger, A., 2007, *Nucleosynthesis and remnants in massive stars of solar metallicity*, *Phys. Rep.*, 442, 269-283
- Woosley, S. E., Weaver, T. A., 1995, *The Evolution and Explosion of Massive Stars. II. Explosive Hydrodynamics and Nucleosynthesis*, *ApJS*, 101, 181
- Zingale, M., Katz, M. P., 2015, *On the Piecewise Parabolic Method for Compressible Flow With Stellar Equations of State*, *ApJS*, 216, 31